Assessment of the electrochemical microcell geometry by local electrochemical impedance spectroscopy of copper corrosion

M. Sanchez, Nizar Aouina, Daniel Rose, Philippe Rousseau, Hisasi Takenouti, Vincent Vivier

Assessment of the electrochemical microcell geometry by local electrochemical impedance spectroscopy of copper corrosion

M. Sánchez[a,b,c,*], N. Aouina[a,b], D. Rose[a,b], P. Rousseau[a,b], H. Takenouti[a,b], V. Vivier[a,b,*]

[a] UPR 15 du CNRS, Laboratoire Interfaces et Systèmes Electrochimiques, 4 place Jussieu, 75252 Paris CEDEX 05, France

[b] Université Pierre et Marie Curie, 4 place Jussieu, 75252 Paris CEDEX 05, France

[c] CISDEM - CSIC, C/ Serrano Galvache 4, 28033 Madrid, Spain

* *Corresponding authors:* mercesanc@ietcc.csic.es (M. Sanchez), vincent.vivier@upmc.fr (V. Vivier)

Abstract

The influence of main geometric parameters of the micro-capillary electrochemical cell such as the capillary diameter and the position of the counter electrode inside the capillary was analysed. For this purpose, Local Electrochemical Impedance Spectroscopy (LEIS) was performed to investigate the corrosion of copper electrode in a dilute sodium chloride aqueous solution using the electrochemical microcell technique. A linear diffusion through a finite diffusion layer was evidenced by LEIS spectra. These experimental data were confronted with digital simulations. It was shown that the diffusion process is taking place through the copper chloride layer on the surface. The capillary diameter and the distance between the counter and the working electrodes are affecting both the thickness and the porosity of the diffusion layer.

Keywords: Microelectrochemistry; Micro-capillary electrode; Local electrochemical impedance spectroscopy (LEIS); Copper corrosion; Finite diffusion layer.

1. Introduction

A family of powerful tools for the investigation of spatially distributed corrosion kinetics was proposed with scanning probe techniques such as the scanning electrochemical microscopy (SECM) [1-6] and the scanning vibrating electrode technique (SVET) [7-9]. Another approach, where a local process predominates on the area under investigation, consists in diminishing the size of the investigated area by miniaturizing the electrochemical cell. Both microelectrodes of small embedded wires [10-14] and capillary-based microcell [14-22] provide valuable information since all common electrochemical measurements can be implemented for these local techniques. In this way, the direct evaluation of local corrosion processes becomes easier.

The basic idea of using capillaries is to address a tiny area on a larger investigated surface well delimited by the capillary diameter [21,22]. Some possibilities and limitations of this technique were already reported by different authors [22-28]. For instance, the concomitant use of the electrochemical microcell and LEIS (local electrochemical impedance spectroscopy) to study corrosion processes was reported in several papers for various metals and alloys [29-34]. In addition, the evaluation of the effect of the microcell geometry on the electrode response presents great interest to avoid the misunderstanding of the local electrochemical measurements obtained with the microcell. However, scarce information concerning the influence of the microcell geometry on the electrode response was reported [26-28].

The present work is aimed at evaluating the influence of the micro-capillary diameter and that of the counter-electrode position inside the microcell on the LEIS measurements to investigate the electrochemical response in the sub-millimetric range. For this purpose, the corrosion of copper was studies as a model-system.

Indeed, copper is one of most extensively employed metals [35-42]. Many studies concerning the corrosion behaviour of copper when exposed to aggressive media such as chloride-containing environments were already reported and the mechanism of copper corrosion in presence of chloride was widely discussed from electrochemical studies on conventional sized electrodes [43-48]. It is worth to notice that the electrochemical behaviour of copper was assessed with the electrochemical microcell both by local polarization curves [49] and by LEIS [14].

2. Experimental conditions

A copper electrode (5 mm in diameter, 99.99% in purity, Goodfellow) was used to study its corrosion behaviour in presence of chloride (0.1 M NaCl solution at room temperature). Electrochemical impedance spectroscopy (EIS) was used to evaluate the electrochemical response of the copper electrode. Both conventional and local electrochemical measurements were investigated. Conventional EIS measurements were performed on the entire copper electrode exposed to the chloride solution in an electrochemical cell with a usual three-electrode configuration: the copper electrode as working electrode, a 1.6 mm in diameter platinum wire surrounding the cell as counter-electrode, and a saturated calomel electrode (SCE) as reference electrode.

Local electrochemical impedance spectroscopy (LEIS) was performed with the electrochemical microcell on the same copper electrode used for conventional measurements. A 0.1 M NaCl solution at room temperature was also used for all the experiments. The electrochemical microcell, already described elsewhere [14], consisted in a micro-capillary fixed to a PMMA (poly(methyl methacrylate)) carrier that also served as electrolyte cell (*c.a.* 0.9 mL), as sketched in Fig. 1a. The working surface

area was delimited by the inner micro-capillary diameter. Commercial micro-capillaries (300 and 500 μm in diameter) pre-treated with silanes were used as received. A homogeneous silicone sealant was formed at the open-end of the capillary tip to ensure a well-reproducible wetted area and to minimize both the leakage and the evaporation of electrolyte. The PMMA carrier also contained the reference electrode, which consisted of a 160 μm in diameter Ag wire previously anodized in KCl solution [50], and the counter-electrode located in the channel of the capillary. This electrode was made of a platinum wire of 100 μm in diameter passing through the carrier. The electrolyte supply was automated by a syringe pump to ensure the complete filling of electrolyte in the capillary. The PMMA carrier was fixed to a strain gauge for controlling a constant mechanical pressure to the silicone sealant. Fig. 1b shows a photography of this home-made experimental setup.

<Fig. 1>

Before each measurement the electrode surface was abraded with emery paper up to the 1200 grade, washed with acetone and rinsed with double deionised water. The polished copper microstructure after etching in 15% NH_3 – 0.5% H_2O_2 solution for 30 s at 25°C revealed, as shown in the SEM picture (Fig. 2), grain size of few tens micrometers, that is, smaller than the capillary diameter used in this work.

<Fig. 2>

All the electrochemical impedance measurements were performed at the open-circuit potential after its stabilization, *i.e.* about 15 minutes. The measurements were carried out with a home-made low-noise potentiostat that allows measurements of high impedance (small current). The impedance measurements were carried out in the 10^5 to 10^{-1} or 10^{-2} Hz frequency range with 7 points per decade. The amplitude of the sinewave perturbation was 20 mV peak to peak (7 mV rms). Both the potential

perturbation and the measurements were made with an analog/digital acquisition device (National Instrument) controlled by a software developed in the laboratory.

3. Results and discussion.

3.1 Measurement of the global electrochemical impedance.

Experimental Nyquist and Bode plots corresponding to conventional EIS (global EIS) measurements, carried out at the corrosion potential on the whole copper electrode are presented in Fig. 3.

<Fig. 3>

EIS data exhibit a capacitive behaviour in the whole frequency domain. According to [45], this electrochemical impedance response can be ascribed to the formation of a porous film of Cu_2O on the copper surface and the dissolution of copper with formation of a CuCl layer controlled by the transport of $CuCl_2^-$ through both the Cu_2O film and the electrolyte. This EIS diagram will be used in the following as reference spectra for the comparison between local and global electrochemical impedances.

3.2 Measurements of LEIS of copper with the electrochemical microcell.

The suitability of the electrochemical microcell to measure the local electrochemical impedance of copper corroding in chloride solutions was shown in a previous study [14]. In the present work, the influence of different parameters of the electrochemical microcell geometry on the electrochemical response was investigated. Among them, both the micro-capillary diameter and the distance between the counter electrode and

the working electrode are parameters that may influence the impedance response of the copper corrosion in presence of chloride.

3.2.1. Influence of the micro-capillary diameter.

The influence of the micro-capillary diameter on EIS is illustrated in Fig. 4 with Nyquist diagram for two different diameters. In these experiments, the counter-electrode was located close to the working electrode surface, that is, at 0.2 mm.

<Fig. 4>

The presence of a small capacitive loop in the high frequency domain (above 1 kHz as shown in the inset of Fig. 4) and the bounded diffusion impedance behaviour in the medium frequency domain (1 kHz – 10 Hz) can be noticed. Above 10 Hz, a similar diagram shape is obtained independently of the micro-capillary diameter. At lower frequencies (f < 1 Hz) a decrease of the real component, often ascribed to an inductive loop, can be observed. However, this apparent inductive loop was not observed on global impedance response with a large surface area. It can be recalled that this inductive behaviour is often attributed to the effect of localized corrosion on the general faradic response of the passive surface [51] as the occurrence of local corrosion processes induces an increase of the active surface area during the electrochemical measurement. Besides, with a larger capillary, the decrease of the real part in the low frequency domain is less marked in agreement with the absence of this phenomenon with the global electrode. The Kramer-Krönig transformation of the both experimental spectra applied to estimate the real component from the imaginary one [52,53] shows a significant divergence between the experimental and the calculated data for frequencies lower than 10 Hz, as can be observed in Fig. 5.

<Fig. 5>

The calculated diagrams do not exhibit the inductive behaviour, but only bounded diffusion impedance below 1 kHz. In this sense, the non-causality of the system, identified from the Kramer-Krönig analysis for frequencies smaller than 10 Hz confirms the evolution of the electrochemical system with time. Though the open circuit potential reaches the steady-state before collecting the impedance spectra, the system is not yet at its steady-state. It is important to emphasize that the presence of pits was observed at the electrode surface where micro-capillary experiments was carried out. It should also be mentioned that that with the larger capillary diameter, the size of the diffusion impedance is greater if the impedance is plotted for the unit surface area (Ω cm^2) whereas it is smaller as observed (in Ω). This phenomenon was also obtained with digital simulation of planar diffusion in micro-capillary electrode as shown below (*see* Fig. 8).

The electrode kinetics examined in term of time constant defined as the apex of the diffusion impedance is also dependent on the capillary size. The greater is the electrode surface area, the smaller is the time constant. The micro-capillary geometry seems to influence the diffusion processes involved in the copper corrosion process.

3.2.2. Influence of the counter electrode position

The effect of the distance between the counter electrode, located inside the micro-capillary, and the working electrode was studied with two micro-capillaries of similar diameter ($\phi \approx 300$ μm). The corresponding Nyquist plots are shown in Fig. 6.

<Fig. 6>

Independently of the distance between the counter and the working electrodes similar impedance diagrams, both in shape and in amplitude, were obtained with the

microcell. However, an increase of the distance between the counter electrode and the working electrode decreases the frequency distribution at which the different processes are revealed.

In addition, the decrease of the real component is also observed at the lowest frequencies (f < 10 Hz) similarly to that observed with shorter distance between the counter and the working electrodes and for different capillary diameters as shown in Fig. 4. The Kramers-Krönig transform analysis also confirms the non-causality of this decrease in the real part at frequencies lower than 10 Hz as presented in Fig. 7.

<Fig. 7>

3.2.3. Influence of microcell geometry on the diffusion process involved

When the LEIS measurements are carried out with the electrochemical microcell, a finite planar diffusion is taking place because the capillary wall does not allow the expansion of the diffusion layer in the radial direction. The FEM calculus of this model assuming a linear diffusion through a finite layer allows taking into account the geometry of the electrochemical system. In Fig. 8 the results of a qualitative digital simulation of the model, supposing generic values for both the concentration and the diffusion coefficient of the diffusing species, are included. A good agreement with the experimental data can be deduced. The changes on the time constants are due to the geometry of the system. It is important to point out that with this type of calculus the distance between the counter and the working electrodes establish the diffusion layer thickness.

<Fig. 8>

The regression calculation of experimental spectra with a simplex algorithm on the basis of the equivalent electric circuit presented in Fig. 9 was performed for the

frequency domain excluding the domain spoiled by experimental error. The impedance of this electrical circuit is given by

$$Z(\omega) = R_e + \frac{R_t + Z_d(\omega)}{1 + (j\omega Q)^{\alpha_d}\left[R_t + Z_d(\omega)\right]} \quad (1)$$

where each element has a following physical meaning: R_e is the electrolyte resistance between the working and the counter electrode, R_t is the charge transfer resistance, Q is the interface CPE (constant phase element) and Z_d is the bounded diffusion impedance. The α_d parameter is employed to take into account the depletion of the capacitive loop at the higher frequencies maybe associated with the porous nature of the copper oxide layer.

<Fig. 9>

A good agreement was found between the experimental and calculated spectra in the selected frequency domain as shown in Fig. 10.

<Fig. 10>

In this figure, experimental data are represented by opened circles and the calculated spectra by crosses. The dotted lines indicate the extrapolation of the calculated spectra. The values determined for each element of the electric circuit are summarized in Table 1. Although not shown in Table 1, a small value for the Cole-Cole coefficient, α_d, was obtained in all cases ($\alpha_d \approx 0.6$) as the capacitive loop at high frequencies is markedly flattened.

<Table 1>

The CPE values obtained for Q indicate that this variable may be associated to the double layer capacitance with the influence of the oxide layer formed on the copper surface. The effect of oxide layer seems to be more marked for smaller micro-capillary. The influence of the capillary on the capacitance values cannot be ruled out as higher capacitance values are obtained for higher distance between the counter electrode and the working electrode maybe due to a capacitive effect on the walls of the capillary. Further studies will be carried out to evaluate this hypothesis.

A fast charge transfer process can be deduced from the small values of R_t obtained.

The bounded diffusion impedance is represented by equation (2) for the pulsation ω.

$$Z_d = R_d \cdot \frac{\tanh(j \cdot \omega \cdot \tau_d)}{\sqrt{j \cdot \omega \cdot \tau_d}} \tag{2}$$

where the diffusion time constant (τ_d) is determined by the thickness of the diffusion layer (δ) and the diffusion coefficient (D)

$$\tau_d = \frac{\delta^2}{D} \tag{3}$$

For a semi-infinite thickness of the diffusion layer, the diffusion impedance can be expressed by the Warburg equation:

$$Z_W = \frac{\sigma}{\sqrt{j \cdot \omega}} \tag{4}$$

Where σ is the Warburg coefficient and can be expressed by the equation (5):

$$\sigma = \frac{R \cdot T}{\sqrt{2} \cdot n^2 \cdot F^2 \cdot C \cdot \sqrt{D} \cdot A} \tag{5}$$

where R is the gas constant (8.31 J mol^{-1} K^{-1}), T the temperature (298 K), n the number of exchanged electrons (n = 2), F the Faraday constant (96500 C mol^{-1}), C the concentration of the diffusing specie (in this case the diffusion of $CuCl_2^-$ was considered and $C = 8.6 \cdot 10^{-7}$ mol cm^{-3} was used) and A the exposed surface area delimited by microcapillary.

The Warburg coefficient, σ, is related with the parameters of the bounded diffusion impedance as:

$$\sigma = \frac{R_d}{\sqrt{\tau_d}} \tag{6}$$

The substitution of equation (6) in equation (5) makes possible the estimation of the diffusion coefficient and then, from the equation (3) the thickness of diffusion layer can be calculated. The estimated values are presented in Table 2.

<Table 2>

The thickness of several micrometers estimated as the diffusion layer in the electrolyte is at least one order of magnitude smaller than that for a large stationary electrode in aqueous medium. With micro-capillary electrode, the thickness is expected to be much greater because the convection is hindered. The thickness in the micrometer range seems reasonable in the case of diffusion in the surface layer of corrosion products, likely the Cu_2O and CuCl layer formed in chloride medium during the corrosion of copper. The thickness of Cu_2O layer in chloride medium in a short immersion period is the order of ten's nm [45], much thinner than that evaluated here. Therefore, the surface involved the diffusion process is essentially CuCl layer. The diffusion coefficient obtained, D, is between two and three orders of magnitude smaller than that of

dissolved oxygen in the bulk solution which is reasonable due to the higher size of the diffusing anion, $CuCl_2^-$. Furthermore, the surface area of open pores through which the anion can diffuse, much smaller than the surface area limited by micro-capillary (A), might favour the smaller values of the diffusion coefficient Both the thickness and the diffusion coefficient are affected by the geometry of the micro-capillary electrode system: a larger diameter of the capillary and also a greater distance between counter electrode and working electrode lead to an increase of both the diffusion layer thickness and the apparent diffusion coefficient. Then, a thicker diffusion CuCl layer induces the frequency shifts towards lower value observed on the impedance diagrams. The origin of the effect of cell geometry upon the thickness of CuCl layer remains yet unknown, and worth to discern them with other experiments or digital modelling.

5. Conclusions

The effects of the electrochemical microcell geometry on the electrode kinetics were studied as a model-system by using the corrosion of copper in chloride aqueous medium since this system is largely studied in the literature. A fast charge transfer process followed by a finite linear diffusion was identified by EIS measurements. On the micro-capillary cell electrode, an inductive-like loop was observed in Nyquist plot. The origin of this phenomenon was attributed, to a non-causal origin to the impedance measurements on the basis of Kramers-Krönig transform, namely the increase of the reaction rate during the impedance measurements induced by pit formation. A large capillary diameter and a long distance between the counter electrode and the working electrode make greater the thickness of the corrosion products formed on the copper electrode surface.

Acknowledgements

The authors gratefully acknowledge F. Pillier (UPR 15 – CNRS) for SEM observations. M. Sánchez acknowledges the Spanish Ministry of Education for her postdoctoral grant.

References

[1] K. Fushimi, M. Seo, Electrochim. Acta 47 (2001) 121-127.

[2] B. Ballesteros Katemann, C. González Inchauspe, P. A. Castro, A. Schultze, E. J. Calvo, W. Schuhmann, Electrochim. Acta 48 (2003) 1115-1121.

[3] N. Casillas, S.J. Charlebois, W.H. Smyrl, H.S. White, J. Electrochem. Soc. 140 (1993) L142.

[4] C. Gabrielli, E. Ostermann, H. Perrot, V. Vivier, L. Beitone, C. Mace, Electrochem. Com. 7 (2005) 962-968.

[5] C. Gabrielli, S. Joiret, M. Keddam, H. Perrot, N. Portail, P. Rousseau, V. Vivier, Electrochim. Acta 52 (2007) 7706-7714.

[6] M. Keddam, N. Portail, D. Trinh, V. Vivier, ChemPhysChem 10 (2009) 3175-3182.

[7] H. S. Isaacs, Corros. Sci. 28 (1988) 547-558.

[8] H. S. Isaacs, J. Electrochem. Soc. 138 (1991) 722-728.

[9] A. M. Simões, A. C. Bastos, M. G. Ferreira, Y. González-García, S. González, R. M. Souto, Corros. Sci. 49 (2007) 726-739.

[10] J. W. Schultze, A. Heidelberg, C. Rosenkranz, T. Schäpers, G. Staikov, Electrochim. Acta 51 (2005) 775-786.

[11] K. Stulik, C. Amatore, K. Holub, V. Marecek, W. Kutner, Pure Appl. Chem. 72 (2000) 1483-1492.

[12] J. Heinze, Angew. Chem. Int. Ed. Engl. 32 (1993) 1268-1288.

[13] Y. I. Tur'yan, Talanta 44 (1997) 1-13.

[14] M. Sanchez, J. Gamby, H. Perrot, D. Rose, V. Vivier, Electrochem. Comm. 12 (2010) 1230-1232.

[15] A. Vogel, J. W. Schultze, Electrochim. Acta 44 (1999) 3751-3759.

[16] V. Vignal, H. Krawiec, O. Heintz, R. Oltra, Electrochim. Acta 52 (2007) 4994-5001.

[17] N. Murer, R. Oltra, B. Vuillemin, O. Néel, Corros. Sci. 52 (2010) 130-139.

[18] H. Krawiec, V. Vignal, R. Oltra, Electrochem. Comm. 6 (2004) 655-660.

[19] H. Krawiec, V. Vignal, R. Akid, Electrochim. Acta 54 (2008) 5252-5259.

[20] E. Dubuisson, P. Lavie, F. Dalard, J. P. Caire, S. Szunerits, Corros. Sci. 49 (2007) 910-919.

[21] H. Böhni, T. Suter, A. Schreyer, Electrochim. Acta 40 (1995) 1361-1368.

[22] M. M. Lohrengel, Corros. Eng. Sci. Technol. 39 (2004) 53-58

[23] T. Suter, H. Böhni, Electrochim. Acta 47 (2001) 191-199.

[24] J. W. Schultze, V. Tsakova, Electrochim. Acta 44 (1999) 3605-3627.

[25] M. M. Lohrengel, A. Moehring, M. Pilaski, Fresenius J. Anal. Chem. 367 (2000) 334-339.

[26] M. M. Lohrengel, A. Moehring, M. Pilaski, Electrochim. Acta 47 (2001) 137-141.

[27] N. Birbilis, B. N. Padgett, R. G. Buchheit, Electrochim. Acta 50 (2005) 3536-3544.

[28] H. Krawiec, V. Vignal, R. Akid, Electrochim. Acta 53 (2008) 5252-5259.

[29] M. Pilaski, T. Hamelmann, A. Moehring, M.M. Lohrengel, Electrochim. Acta 47 (2002) 2127-2134.

[30] M.M. Lohrengel, S. Heiroth, K. Kluger, M. Pilaski, B. Walther, Electrochim. Acta 51 (2006) 1431-1436.

[31] H. Krawiec, V. Vignal, O. Heintz, R. Oltra, Electrochim. Acta 51 (2006) 3235-3243.

[32] H. Krawiec, V. Vignal, J. Banas, Electrochim. Acta 54 (2009) 6070-6074.

[33] J.B. Jorcin, H. Krawiec, N. Péberè, V. Vignal, Electrochim. Acta 54 (2009) 5775-5781.

[34] E. Dubuisson, P. Lavie, F. Dalard, J.P. Caire, S. Szunerits, Electrochem. Comm. 8 (2006) 911-915.

[35] G. Bengough, R. Jones, R. Pirret, J. Inst. Met. 23 (1920) 65.

[36] A. L. Bacarella, J. C. Griess, J. Electrochem. Soc. 120 (1973) 459-465.

[37] C. H. Bonfiglio, H. C. Albaya, O. A. Cobo, Cor. Sci. 13 (1973) 717-724.

[38] D. W. Shoesmith, T. E. Rummery, D. Owen, W. Lee, J. Electrochem. Soc. 123 (1976) 790-799.

[39] H. P. Lee, K. Nobe, A. J. Pearlstein, J. Electrochem. Soc. 132 (1985) 1031-1037.

[40] V. Brusic, M. A. Frisch, B. N. Eldridge, F. P. Novak, F. B. Kaufman, B. M. Rush, G. S. Frankel, J. Electrochem. Soc. 138 (1991) 2253-2259.

[41] O. E. Barcia, O. R. Mattos, N. Pébère, B. Tribollet, J. Electrochem. Soc. 140 (1993) 2825-2832.

[42] R. Babic, M. Metikos-Hukovic, A. Jukic, J. Electrochem. Soc. 148 (2001) B146-B151.

[43] G. Bianchi, P. Longhi, Corros. Sci. 13 (1973) 853-864..

[44] C. Deslouis, M. M. Musiani, C. Pagura, B. Tribollet, J. Appl. Electrochem. 18 (1988) 374-383.

[45] C. Deslouis, M. M. Musiani, C. Pagura, B. Tribollet, J. Appl. Electrochem. 18 (1988) 384-393.

[46] E. D'Elia, O.E. Barcia, O.R. Mattos, N. Pébère, B. Tribollet, J. Electrochem. Soc. 143 (1996) 961-967.

[47] B. Trachli, M. Keddam, H. Takenouti, A. Shriri, Corros. Sci. 44 (2002) 997-1008.

[48] G. Kear, B.D. Barken, F.C. Walsh, Corros. Sci. 46 (2004) 109-135.

[49] J. Gravier, V. Vignal, S. Bissey-Breton, J. Farre, Corros. Sci. 50 (2008) 2885-2894.

[50] C. Gabrielli, S. Joiret, M. Keddam, H. Perrot, N. Portail, P. Rousseau, V. Vivier, J. Electrochem. Soc. 153 (2006) B68-B74.

[51] R. Oltra, M. Keddam, Corros. Sci. 28 (1988) 1-18.

[52] C. Gabrielli, M. Keddam, H. Takenouti, Kramers-Krönig transformation in relation to the interface regulating device, in: Electrochemical Impedance: Analysis and Interpretation, ASTM STP 1188, J. R. Scully, D. C. Silverman, M. W. Kending (Eds.), American Society for Testing and Materials, Philadelphia, 1993, pp. 140-153.

[53] P. Agarwal, M. E. Orazem, L. H. Garcia-Rubio, Application of the Kramers-Krönig relations in electrochemical impedance spectroscopy, in: Electrochemical Impedance: Analysis and Interpretation, ASTM STP 1188, J. R. Scully, D. C. Silverman, M. W. Kending (Eds.), American Society for Testing and Materials, Philadelphia, 1993, pp. 115-139.

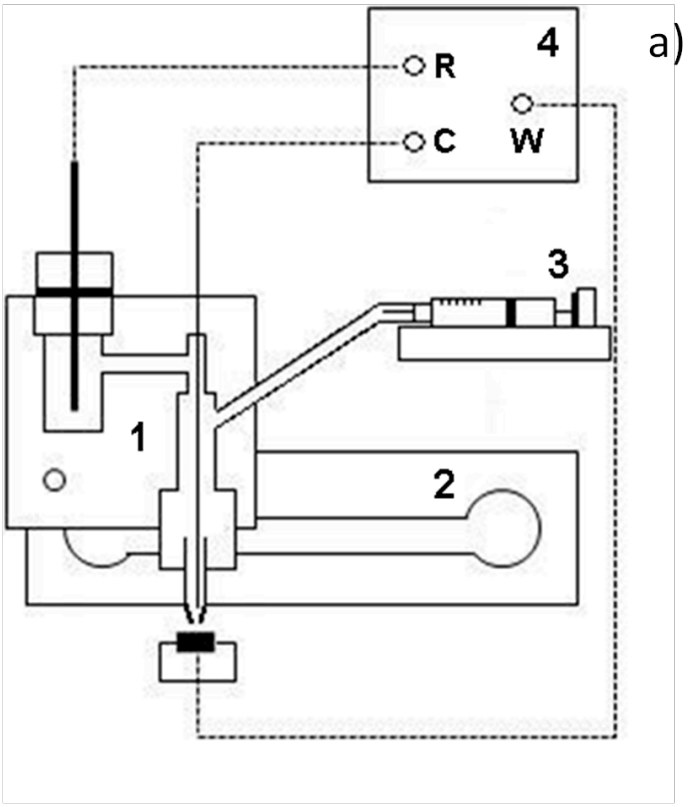

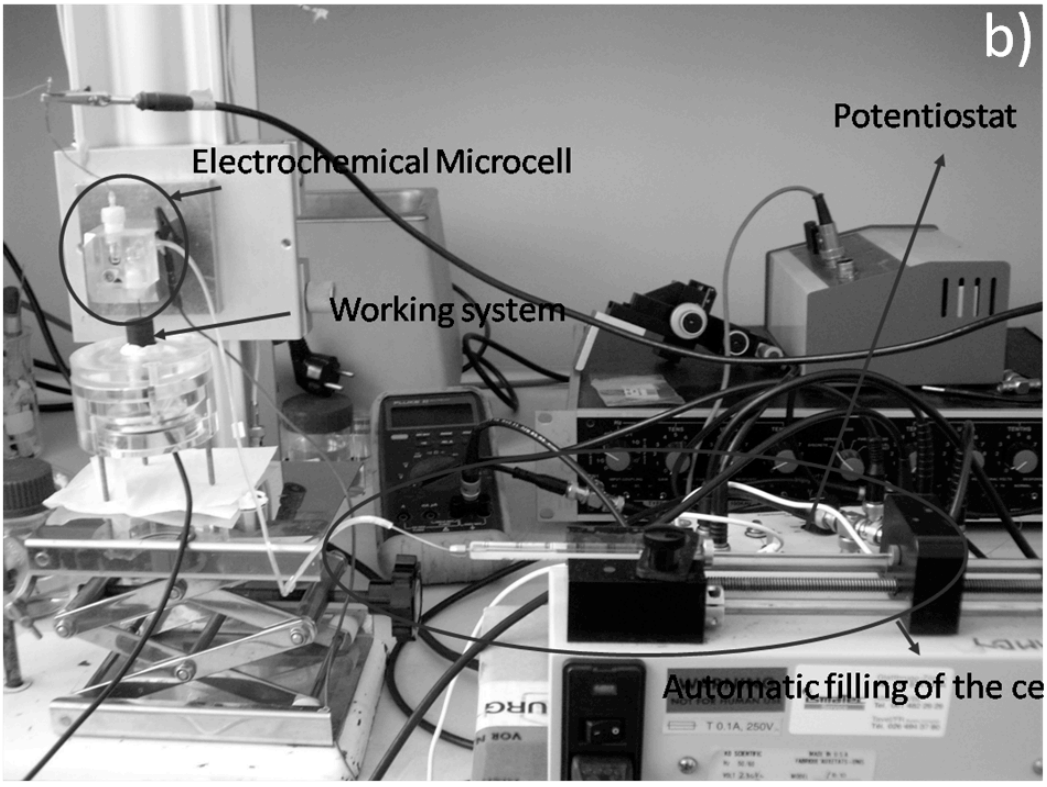

Fig. 1. (a) Sketch of the setup of the electrochemical microcell system. 1) Microcell with the capillary, 2) Strain gauge, 3) Syringe pump, 4) Potentiostat (C (counter electrode), R (reference electrode), W (working electrode)); (b) Picture of the whole home-made setup.

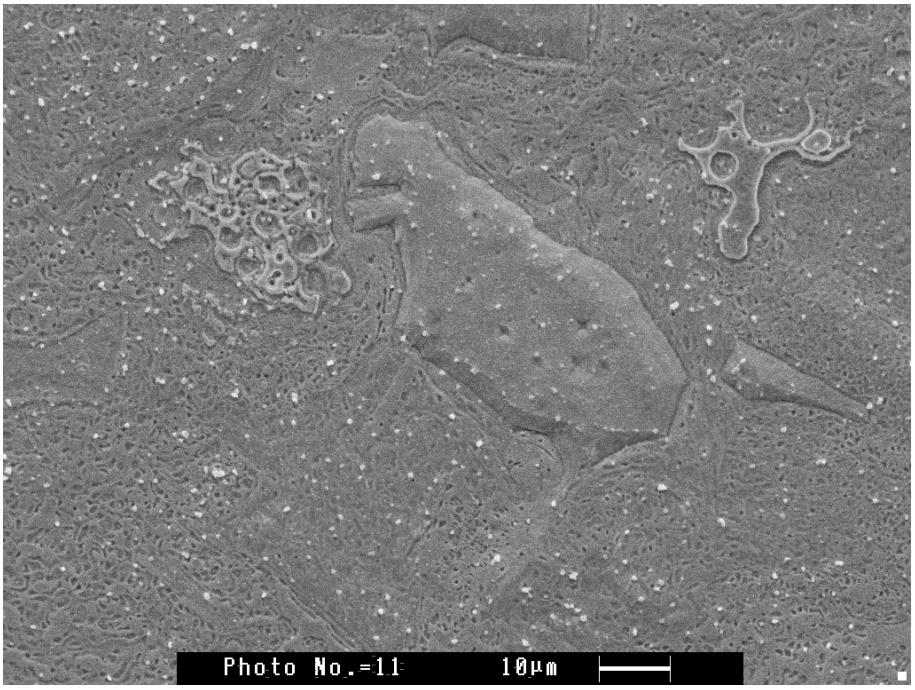

Fig. 2. Metallographic observation of the Cu microstructure with SEM.

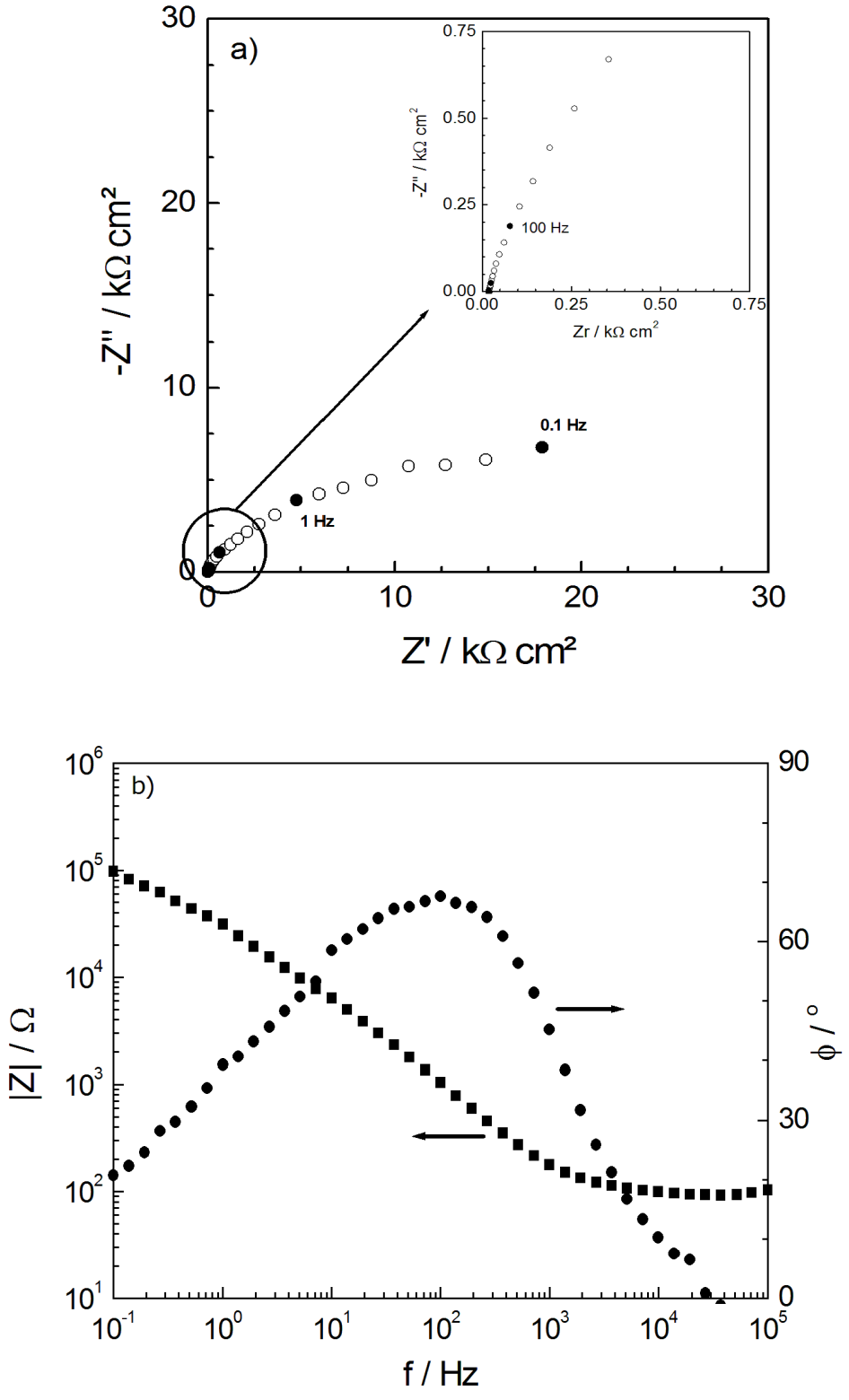

Fig. 3. Global EIS measurement on a copper electrode (5 mm in diameter) in 0.1 M NaCl solution: (a) Nyquist diagram; (b) Bode diagram.

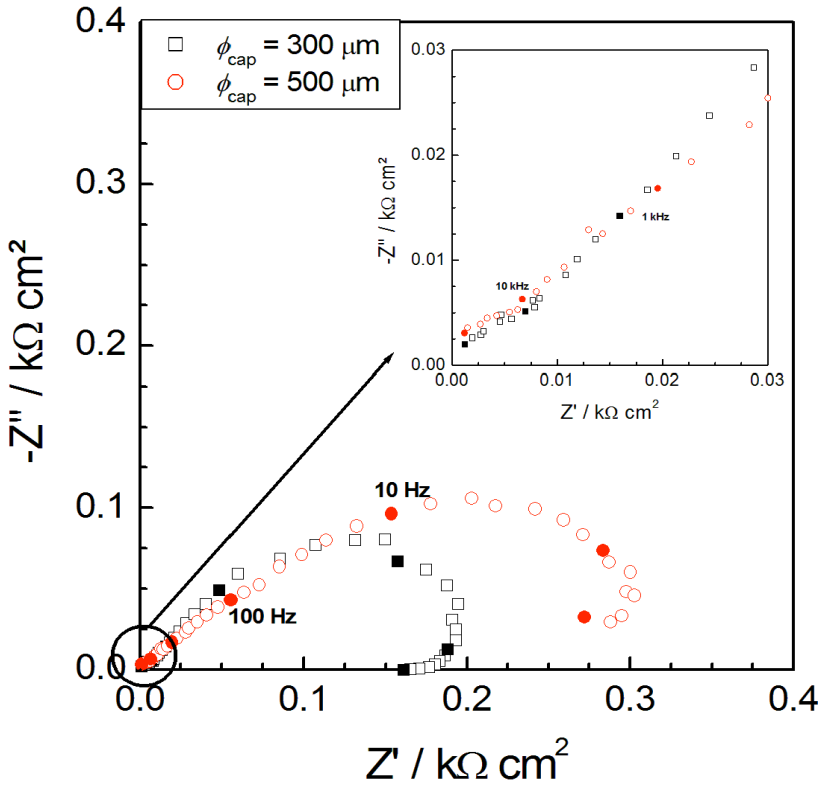

Fig. 4. Influence of the capillary diameter on the LEIS response of copper electrode in 0.1 M NaCl. The experiments were performed with the same distance between the counter and the working electrodes ($d_{CE\text{-}WE}$ = 0.2 mm).

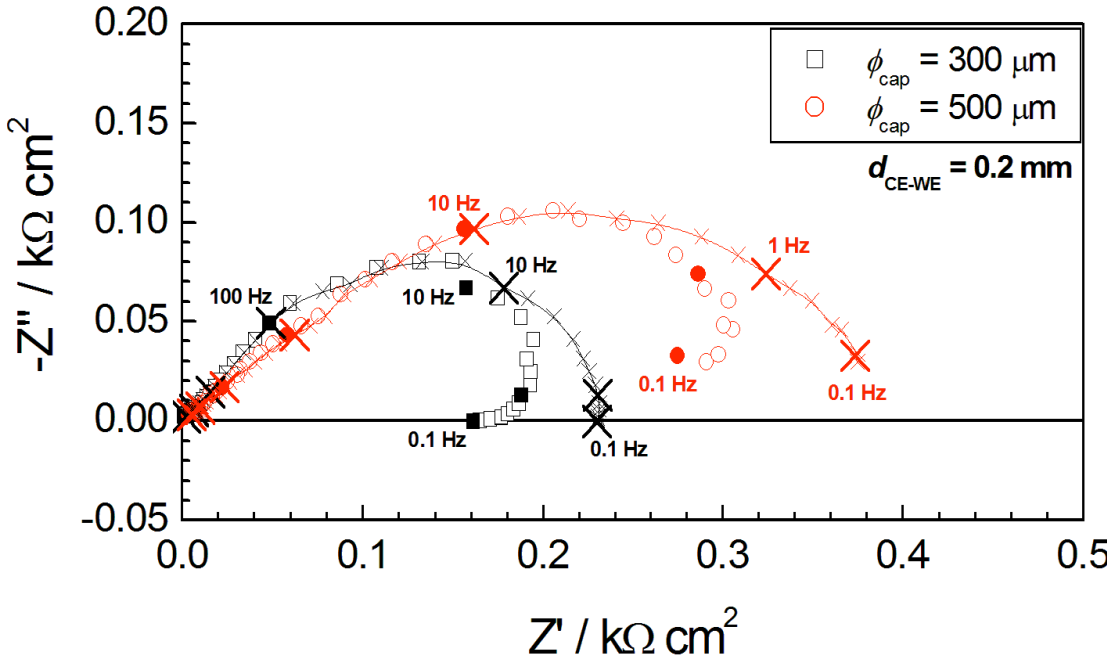

Fig. 5. Kramers-Krönig transforms of experimental impedance spectra from Fig. 4. Calculations were performed from the imaginary part.

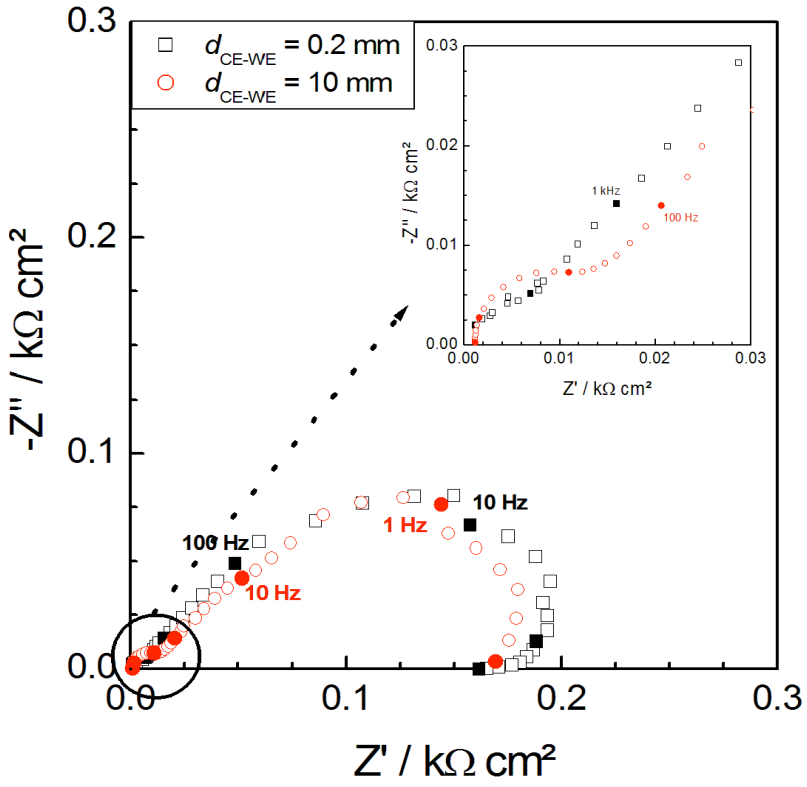

Fig. 6. Influence of the distance between the counter electrode and the working electrode on LEIS measurements on copper in 0.1 M NaCl performed with the electrochemical microcell ($\phi \approx 300$ µm).

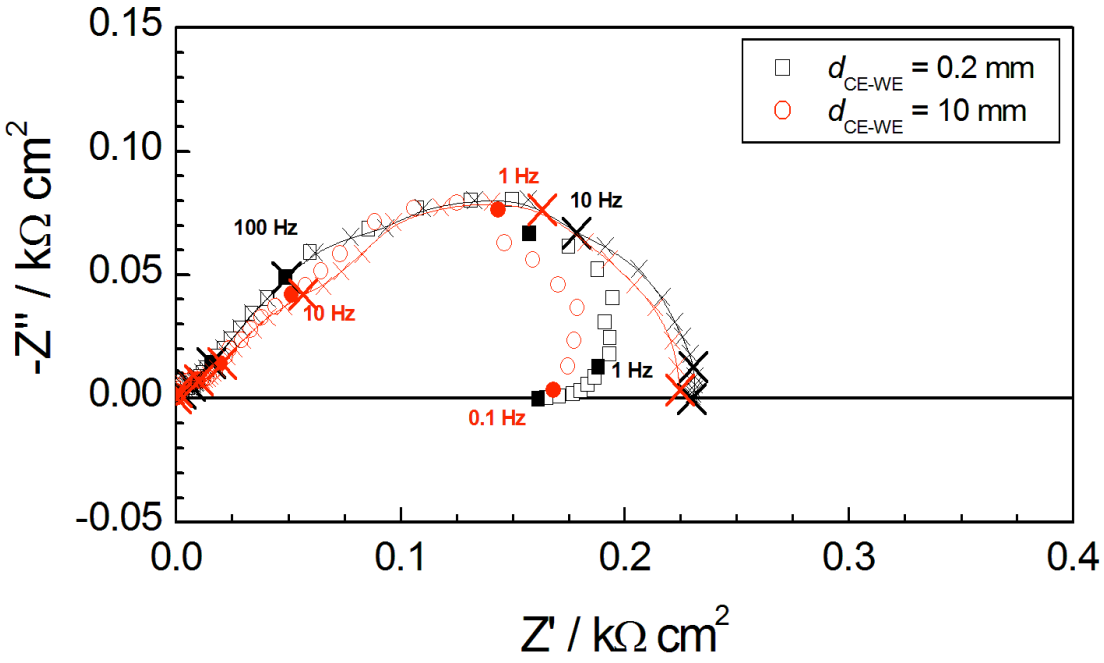

Fig. 7. Kramers-Krönig transforms of experimental impedance spectra performed with microcapillaries of 300 μm in diameter and different distances between the counter and the working electrodes.

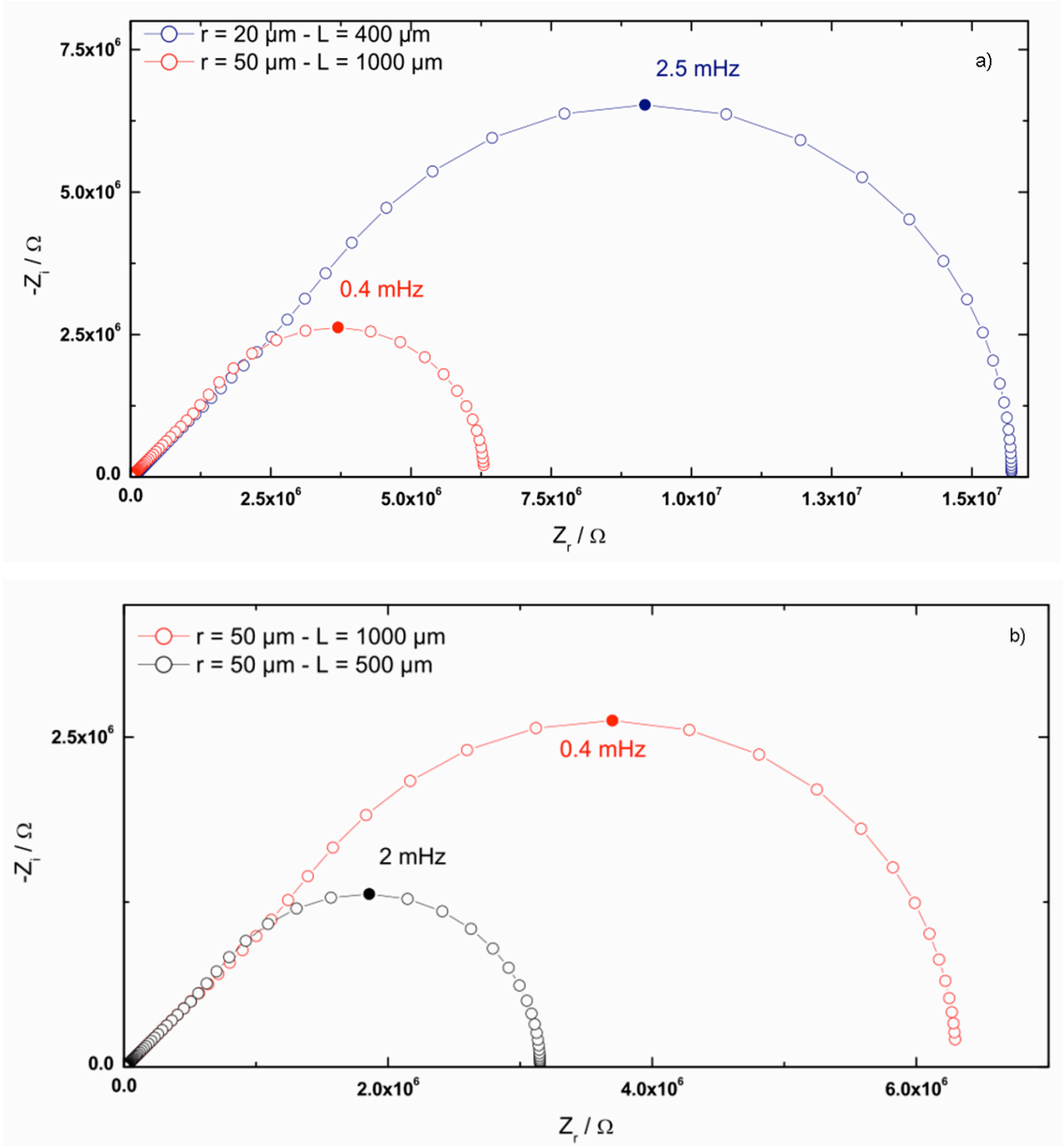

Fig. 8. Digital simulation of LEIS measurements performed with the microcell (assuming a linear diffusion through a finite layer, $D = 10^{-6}$ cm^2·s^{-1}, $C = 10^{-5}$ mol/cm^{-3}): a) Influence of the microcapillary diameter (r), b) Influence of the distance between the counter and the working electrodes (L).

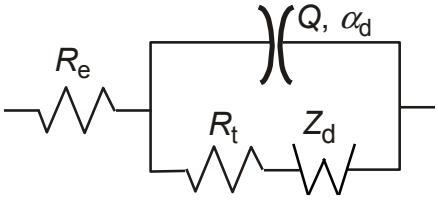

Fig. 9. Electric equivalent circuit used for determining the parameters with a simplex algorithm. Input parameters: R_e - electrolyte resistance; C_d double layer capacitance, and α_d - coefficient representing a flattened feature of capacitive response; R_t - charge transfer resistance; Z_d - bounded diffusion impedance.

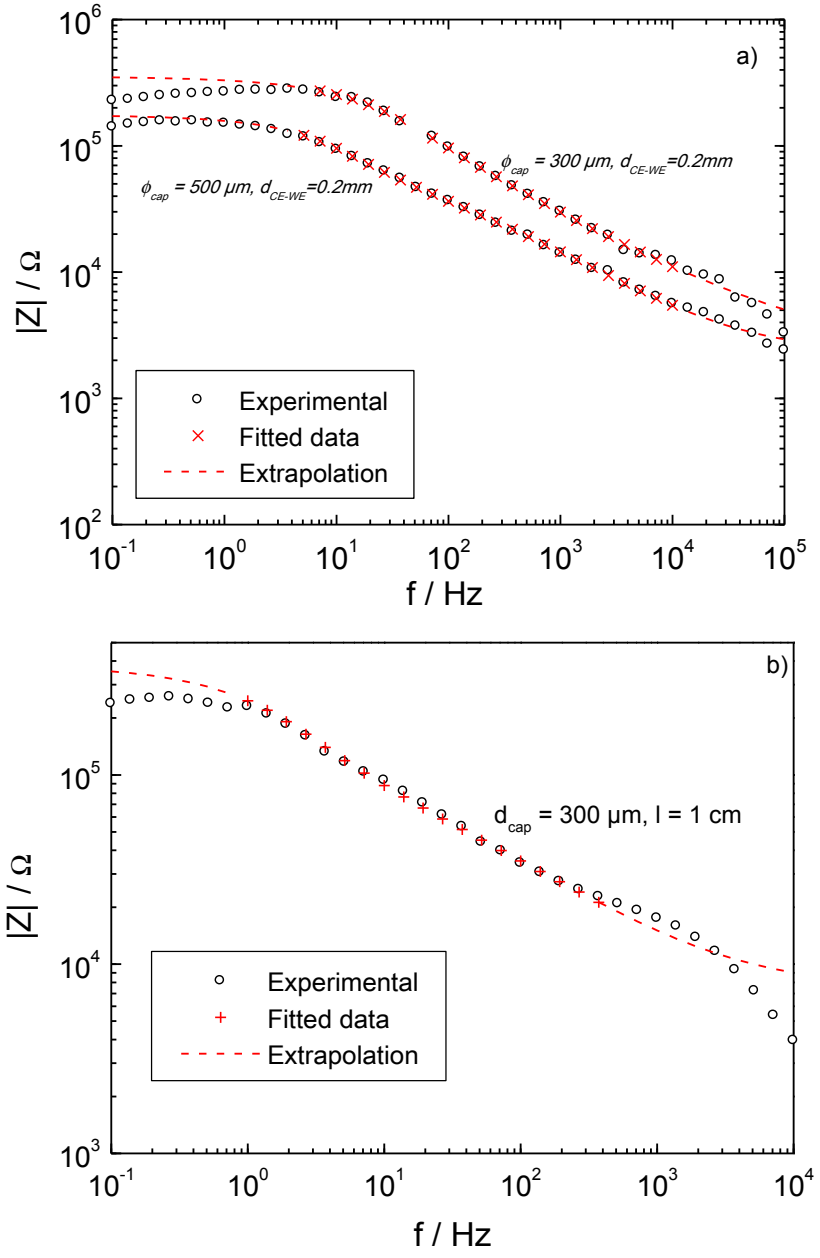

Fig. 10. Fitting of experimental LEIS with simplex algorithm using the equivalent electric circuit of Fig. 8. (a) Different diameter of the microcapillary with small distance between the counter and the working electrodes (d_{CE-WE} = 0.2 mm), (b) Large distance between the counter and the working electrodes (d_{CE-WE} = 10 mm).